Research

CrossMark
click for updates

Author for correspondence:
Paolo Falsaperla
e-mail: falsaperla@dmi.unict.it

Bidispersive-inclined convection

Paolo Falsaperla[1], Giuseppe Mulone[1] and
Brian Straughan[2]

[1]Dipartimento di Matematica e Informatica, Città Universitaria,
Viale A. Doria, 6, 95125 Catania, Italy
[2]Department of Mathematical Sciences, University of Durham,
Durham DH1 3LE, UK

PF, 0000-0001-7184-9798

A model is presented for thermal convection in an inclined layer of porous material when the medium has a bidispersive structure. Thus, there are the usual macropores which are full of a fluid, but there are also a system of micropores full of the same fluid. The model we employ is a modification of the one proposed by Nield & Kuznetsov (2006 *Int. J. Heat Mass Transf.* **49**, 3068–3074. (doi:10.1016/j.ijheatmasstransfer.2006.02.008)), although we consider a single temperature field only.

1. Introduction

Thermal convection in an inclined layer is a subject that has attracted much attention. For the situation where the layer is full of a Newtonian fluid a comprehensive analysis is provided by Chen & Pearlstein [1], who also give a lucid historical review of work prior to their article. Recently, many authors have been investigating thermal convection in a fluid-saturated, inclined porous layer, or even a vertical layer, see e.g. Barletta [2], Barletta & Celli [3], Barletta & Storesletten [4] and Barletta & Rees [5]; the last-mentioned contribution contains a good review of earlier work.

In this article, we shall commence an analysis of thermal convection in a fluid-saturated porous layer but when the porous material is of bidispersive type. Bidispersive porous materials were introduced theoretically in the late 1990s, e.g. Nield [6,7], Nield & Bejan [8], Nield & Kuznetsov [9] and chapter 13 of Straughan [10]. See also the recent paper by Nield [11]. A bidispersive porous medium is one where there are pores of the usual type which are referred to as macropores. Associated with the macropores is the

porosity ϕ which is the ratio of the volume of the macropores to the total volume of saturated porous material.

However, in the solid skeleton, there are much smaller micropores, e.g. the picture given in Nield & Kuznetsov [9, p. 3069]. Attached to the micropores is a porosity ϵ which is the ratio of the volume occupied by the micropores to the volume of the porous body that remains once the macropores are removed. Thus, the fraction of volume occupied by the micropores is $\epsilon(1 - \phi)$, whereas the fraction occupied by the solid skeleton is $(1 - \epsilon)(1 - \phi)$. Nield & Kuznetsov [9] gave a comprehensive analysis of linear instability for thermal convection in a bidispersive porous material when the layer is horizontal. They allowed for different velocities U_i^f and U_i^P in the macro- and micropores and also catered for different fluid temperatures T^f and T^P in the macro and micropores. Our goal is here to assess the effect of induced velocity owing to inclination and gravity upon instability, and so we here restrict attention to a single temperature T, although we do follow Nield & Kuznetsov [9] and allow different macro- and micropore velocities U_i^f and U_i^P.

We should point out that bidispersive porous materials (or double porosity materials) are very important and are the subject of intense recent research owing to the many real-life application areas. For example, bidispersive porous media are crucial to understanding the physics of underground drinking water supplies [12,13]; they are also crucial to understanding the highly controversial topic of hydraulic fracturing (or 'fracking') in which rocks underground are deliberately vibrated to release trapped natural gas [14,15]. Other application areas are given in Straughan [10]. A further area of particular interest for thermal convection in an inclined plane is to landslides [16] or more generally land deformation involving thermal gradients [17,18].

In §2, we introduce the basic equations for thermal convection in a bidispersive porous medium. In particular, we derive the energy balance law when a single temperature is employed. In the section following, we derive the basic solution for thermal convection in an inclined layer. The section following that analyses linear instability in detail. The penultimate section presents some global stability results when the fully nonlinear theory is employed. The final section is reserved for conclusions.

2. Basic equations

Let U_i^f and U_i^P be the velocity fields in the macro- and micropores, respectively. The momentum equations governing the evolutionary behaviour of the velocity fields are taken from Nield & Kuznetsov [9], equations (1) and (2), but we omit the Brinkman terms and we additionally have only one temperature field, T. Thus, setting $T^f = T^P = T$ in equations (6)–(10) of Nield & Kuznetsov [9] and omitting the Brinkman terms, the equations for U_i^f and U_i^P are

and

$$\left. \begin{aligned} -\frac{\mu}{K_f} U_i^f - \zeta(U_i^f - U_i^P) - p_{,i}^f - \rho_F \hat{\beta} T g_i &= 0 \\ -\frac{\mu}{K_P} U_i^P - \zeta(U_i^P - U_i^f) - p_{,i}^P - \rho_F \hat{\beta} T g_i &= 0. \end{aligned} \right\} \tag{2.1}$$

In these equations, μ is the fluid viscosity, K refers to permeability, ζ is an interaction coefficient, p refers to the pressures and sub/superscript 'f' and 'p' refer to macro and micropore effects. In addition, $\hat{\beta}$ is the thermal expansion coefficient and T_F is a reference temperature where the buoyancy term involves a linear density of form

$$\rho = \rho_F(1 - \hat{\beta}(T - T_F)).$$

We have also used g_i to denote the gravity vector.

We suppose that the porous material occupies an inclined plane with angle from the vertical δ, where $0 \leq \delta \leq \pi/2$ radians, cf. the geometrical configuration of Chen & Pearlstein [1]. Thus, in our case,

$$\mathbf{g} = -g(\cos \delta, 0, \sin \delta),$$

where, as in Chen & Pearlstein [1], x is measured in the longitudinal direction along the layer, z is orthogonal, with the boundaries being at $z = 0$ and $z = d$, and **g** is gravity.

To derive the energy balance equation governing the behaviour of the temperature field, we generalize the procedure of Joseph [19], see also Straughan [20, p. 47] and [10, p. 16] . Let V be a representative elementary volume, REV, and denote by s, f and p the properties of the solid skeleton, macropores and micropores, respectively. Let V_i^f and V_i^p be the actual velocities in the macro- and micropores. Then, we may write equations for the separate temperature fields T^s, T^f and T^p as

$$(\rho c)_s T^s_{,t} = \kappa_s \Delta T^s,$$
$$(\rho c)_f T^f_{,t} + (\rho c)_f V_i^f T^f_{,i} = \kappa_f \Delta T^f + h(T^p - T^f)$$
$$(\rho c)_p T^p_{,t} + (\rho c)_p V_i^p T^p_{,i} = \kappa_p \Delta T^p + h(T^f - T^p),$$

and

$$\tag{2.2}$$

where ρ and c refer to density and specific heat at constant pressure, κ is the thermal conductivity and h is a temperature interaction coefficient. Throughout, we employ standard indicial notation, and Δ is the *Laplace* operator. We have followed Nield & Kuznetsov [9] and employed interactions between T^f and T^p. We could also include interactions between T^s and T^f or T^s and T^p.

In the next step, we multiply $(2.2)_1$ by $(1 - \phi)(1 - \epsilon)$, $(2.2)_2$ by ϕ and $(2.2)_3$ by $\epsilon(1 - \phi)$, and add the results, setting $T^s = T^f = T^p = T$.

In the REV, we thus have, recalling $U_i^f = \phi V_i^f$ and $U_i^p = \epsilon(1 - \phi)V_i^p$ are the pore averaged velocities,

$$(\rho c)_m T_{,t} + (\phi_1 U_i^f + \phi_2 U_i^p)T_{,i} = \kappa_m \Delta T,$$

where

$$(\rho c)_m = (1 - \phi)(1 - \epsilon)(\rho c)_s + (\rho c)_f \phi + \epsilon(1 - \phi)(\rho c)_p$$
$$\phi_1 = (\rho c)_f, \quad \phi_2 = (\rho c)_p$$

and

$$\kappa_m = (1 - \phi)(1 - \epsilon)\kappa_s + \phi \kappa_f + \epsilon(1 - \phi)\kappa_p.$$

We have followed Nield & Kuznetsov [9] and allowed $(\rho c)_f$ and $(\rho c)_p$ to be different. Because Nield & Kuznetsov dealt with different macro- and micropore temperatures, it is possible $(\rho c)_f$ and $(\rho c)_p$ will be different. However, in the present case of single temperature, we expect that as the macro- and micropores are composed of the same fluid $(\rho c)_f$ and $(\rho c)_p$ will be the same. Thus, in our case, we may simplify equations (2.1) and (2.2), and we work with the system

$$-\frac{\mu}{K_f} U_i^f - \zeta(U_i^f - U_i^p) - p^f_{,i} - \rho_F \hat{\beta} T g_i = 0,$$
$$-\frac{\mu}{K_p} U_i^p - \zeta(U_i^p - U_i^f) - p^p_{,i} - \rho_F \hat{\beta} T g_i = 0$$

and

$$(\rho c)_m T_{,t} + \phi_1(U_i^f + U_i^p)T_{,i} = \kappa_m \Delta T,$$

$$\tag{2.3}$$

where now

$$(\rho c)_m = (1 - \phi)(1 - \epsilon)(\rho c)_s + [\phi + \epsilon(1 - \phi)](\rho c)_f.$$

Thus, the fundamental equations governing the behaviour of U_i^f, U_i^p and T in a Darcy bidispersive porous medium with a single temperature may be taken to be (2.3).

3. Perturbation equations

From equation (2.3), we seek a basic solution of the form $\bar{\mathbf{U}}^f = (\bar{U}^f(z), 0, 0)$, $\bar{\mathbf{U}}^p = (\bar{U}^p(z), 0, 0)$ and $\bar{T}(z)$, subject to the boundary conditions

$$\bar{T}(0) = T_L, \quad \bar{T}(d) = T_U$$

for constants T_L and T_U. We consider the two cases of heating from above, $T_U > T_L$ and heating from below, $T_L > T_U$. In addition, we normalize the solution by requiring

$$\int_0^d \bar{U}^f(z)\, dz = 0, \quad \int_0^d \bar{U}^P(z)\, dz = 0,$$

cf. Chen & Pearlstein [1]. After transporting the interval $0 \le z \le d$ into $z \in [0,1]$, we find the basic solution in whose stability we are interested is

$$\bar{T} = T_L \pm |\Delta T| z,$$

where the sign $+$ indicates heating from above whereas $-$ denotes heating from below and $|\Delta T| = |T_L - T_U|$.

The basic velocities have form

$$\bar{U}^f = \mp \frac{1}{\varXi}\left(\frac{\mu}{K_p} + 2\zeta\right) g \cos\delta \rho_F \hat{\beta} |\Delta T| \left(\frac{1}{2} - z\right)$$

$$\bar{U}^P = \mp \frac{1}{\varXi}\left(\frac{\mu}{K_f} + 2\zeta\right) g \cos\delta \rho_F \hat{\beta} |\Delta T| \left(\frac{1}{2} - z\right),$$

where the coefficient $\varXi$ is given by

$$\varXi = \frac{\mu^2}{K_f K_p} + \mu\zeta\left(\frac{1}{K_f} + \frac{1}{K_p}\right)$$

and $\mp$ indicates heating from above/below, respectively.

We now introduce perturbations and write

$$U_i^f = \bar{U}_i^f + u_i^f, \quad U_i^P = \bar{U}_i^P + u_i^P, \quad T = \bar{T} + \theta, \quad p^f = \bar{p}^f + \pi^f, \quad p^P = \bar{p}^P + \pi^P.$$

We non-dimensionalize with length scale d, time scale

$$\mathcal{T} = \frac{d^2(\rho c)_m}{\kappa_m},$$

velocity scale

$$U = \frac{\kappa_m}{(\rho c)_m d},$$

temperature scale

$$T^{\#} = U\sqrt{\frac{\mu(\rho c)_m \phi_1 |\Delta T| \mathcal{T}}{d \rho_F \hat{\beta} g K_f}},$$

relative permeability $K_r = K_p/K_f$, Rayleigh number

$$R^2 = Ra = \frac{\phi_1 |\Delta T| \mathcal{T} \rho_F \hat{\beta} g K_f}{d\mu(\rho c)_m},$$

$\sigma_f = \zeta K_f/\mu$ and $\lambda = (\cos\delta, 0, \sin\delta)$. In this manner, we may arrive at the non-dimensional equations

$$\left.\begin{aligned}
-u_i^f - \sigma_f(u_i^f - u_i^P) - \pi_{,i}^f + R\lambda_i\theta &= 0, \\
-u_i^P - K_r\sigma_f(u_i^P - u_i^f) - K_r\pi_{,i}^P + K_r R\lambda_i\theta &= 0
\end{aligned}\right\} \tag{3.1}$$

and

$$\theta_{,t} \pm Rw^f \pm Rw^P \mp R^2\cos\delta(\tfrac{1}{2} - z)N_k\theta_{,x} + K_N(u_i^f\theta_{,i} + u_i^P\theta_{,i}) = \Delta\theta,$$

where the top signs indicate heating from above, whereas the bottom ones signify heating from below, $w^f = u_3^f$, $w^P = u_3^P$, and N_k, K_N are non-dimensional parameters of form

$$N_k = \frac{1 + K_r(1 + 4\sigma_f)}{1 + K_r\sigma_f(1 + K_r)}, \quad K_N = \frac{Ud\phi_1}{K_m}.$$

One may observe that K_N is a sort of thermal Reynolds number.

4. Linear instability

To proceed, we linearize equations (3.1), then remove the pressures π^f and π^P by taking *curlcurl* of equations $(3.1)_{1,2}$. Then, in terms of w^f, w^P and θ, we obtain equations and then introduce normal modes by writing $f = f(z)\,e^{i(ax+by)+ct}$, where f is w^f, w^P and θ, to obtain

$$
\left.
\begin{array}{l}
\mathcal{D}^2 w^f + \sigma_f(\mathcal{D}^2 w^f - \mathcal{D}^2 w^P) + Ria\cos\delta D\theta + R\sin\delta(a^2+b^2)\theta = 0 \\[6pt]
\mathcal{D}^2 w^P + K_r\sigma_f(\mathcal{D}^2 w^P - \mathcal{D}^2 w^f) + K_r R[ia\cos\delta D\theta + \sin\delta(a^2+b^2)\theta] = 0
\end{array}
\right\}
\tag{4.1}
$$

and

and

$$
c\theta \pm Rw^f \pm Rw^P \mp (\tfrac{1}{2}-z)R^2 N_K \cos\delta\, ia\theta = \mathcal{D}^2\theta .
\tag{4.2}
$$

In equations (4.1)–(4.2), $\mathcal{D}^2$ is defined by

$$
\mathcal{D}^2 \equiv D^2 - (a^2+b^2),
$$

where $D = d/dz$.

Equations (4.1)–(4.2) are solved numerically by a Chebyshev tau method [21] with boundary conditions

$$
w^f = 0, \quad w^P = 0, \quad \theta = 0, \quad \text{for } z = 0, 1.
\tag{4.3}
$$

5. Nonlinear stability

In this section, we include a global nonlinear stability result when the inclined layer is heated from above.

We commence with equations (3.1) with the top signs, so that we have

$$
\left.
\begin{array}{l}
-u_i^f - \sigma_f(u_i^f - u_i^P) - \pi_{,i}^f + R\lambda_i\theta = 0, \\[10pt]
-\dfrac{u_i^P}{K_r} - \sigma_f(u_i^P - u_i^f) - \pi_{,i}^P + R\lambda_i\theta = 0, \\[10pt]
\theta_{,t} + Rw^f + Rw^P - R^2\cos\delta\left(\dfrac{1}{2}-z\right)N_k\theta_{,x} + K_N(u_i^f\theta_{,i} + u_i^P\theta_{,i}) = \Delta\theta.
\end{array}
\right\}
\tag{5.1}
$$

and

We suppose that

$$
w^f = w^P = 0, \quad \theta = 0, \quad \text{on } z = 0, 1,
$$

and u_i^f, u_i^P, θ, π^f and π^P satisfy a plane tiling periodicity in x and y, such that the solution has a periodicity cell V.

Multiply $(5.1)_1$ by u_i^f and $(5.1)_2$ by u_i^P and integrate each over V. Likewise multiply $(5.1)_3$ by $\theta\sin\delta$ and integrate over V. After some integrations by parts and use of the boundary conditions, we add the results to obtain the equation

$$
\frac{\sin\delta}{2}\frac{d}{dt}\|\theta\|^2 = R\cos\delta(\theta, u^f + u^P) - \sin\delta\|\nabla\theta\|^2 - \|\mathbf{u}^f\|^2 - \frac{1}{K_r}\|\mathbf{u}^P\|^2 - \sigma_f\|\mathbf{u}^f - \mathbf{u}^P\|^2.
\tag{5.2}
$$

In (5.2), $u^f = u_1^f$, $u^P = u_1^P$, $(\cdot,\cdot)$ and $\|\cdot\|$ are the inner product and norm in $L^2(V)$. It is worth observing that the term involving $\theta_{,x}$ integrates to zero as do the cubic nonlinear terms which arise.

From (5.2), we obtain

$$\frac{\sin \delta}{2} \frac{\mathrm{d}}{\mathrm{d}t} \|\theta\|^2 \leq R \cos \delta(\theta, u^f + u^P) - \sin \delta \|\nabla \theta\|^2 - \|\mathbf{u}^f\|^2 - \frac{1}{K_r}\|\mathbf{u}^P\|^2.$$

Let λ_1 the first eigenvalue in the membrane problem for V (in fact $\lambda_1 = \pi^2$) and then we use the arithmetic–geometric mean inequality to find

$$\frac{\sin \delta}{2} \frac{\mathrm{d}}{\mathrm{d}t} \|\theta\|^2 \leq \left(R \frac{\cos \delta}{2} \left[\frac{1}{\epsilon_1} + \frac{1}{\epsilon_2} \right] - \lambda_1 \sin \delta \right) \|\theta\|^2$$

$$- \|\mathbf{u}^f\|^2 \left(1 - \frac{R\epsilon_1 \cos \delta}{2} \right) - \|\mathbf{u}^P\|^2 \left(\frac{1}{K_r} - \frac{R\epsilon_2 \cos \delta}{2} \right) \tag{5.3}$$

where $\epsilon_1 > 0, \epsilon_2 > 0$ are at our disposal.

We now select $\epsilon_1 = 2/R \cos \delta$ and $\epsilon_2 = 2/K_r R \cos \delta$ and then from (5.3), we obtain

$$\frac{\sin \delta}{2} \frac{\mathrm{d}}{\mathrm{d}t} \|\theta\|^2 \leq - \left(\lambda_1 \sin \delta - R^2 \frac{\cos^2 \delta}{4}[1 + K_r] \right) \|\theta\|^2. \tag{5.4}$$

Thus, provided

$$R^2 < \left(\frac{4\lambda_1}{1 + K_r} \right) \frac{\sin \delta}{\cos^2 \delta}, \tag{5.5}$$

the coefficient at the right-hand side of (5.4) is negative, and this inequality integrates to see that $\|\theta\|$ decays at least exponentially in time. Thus, (5.5) represents a global nonlinear stability threshold.

To establish decay of $\mathbf{u}^f$ and $\mathbf{u}^P$ under (5.5), we employ the relations obtained above to find after using arithmetic–geometric mean inequality

$$\|\mathbf{u}^f\|^2 + K_r^{-1}\|\mathbf{u}^P\|^2 \leq \|\mathbf{u}^f\|^2 + K_r^{-1}\|\mathbf{u}^P\|^2 + \sigma_f\|\mathbf{u}^f - \mathbf{u}^P\|^2$$

$$= R \cos \delta[((\theta, u^f) + (\theta, u^P)] + R \sin \delta[((\theta, w^f) + (\theta, w^P)]$$

$$\leq \frac{1}{2}\|\mathbf{u}^f\|^2 + \frac{1}{2K_r}\|\mathbf{u}^P\|^2 + \frac{R^2}{2}(1 + K_r)\|\theta\|^2. \tag{5.6}$$

Because from (5.5) and (5.4), $\|\theta\|$ decays exponentially, (5.6) demonstrates $\|\mathbf{u}^f\|$ and $\|\mathbf{u}^P\|$ likewise have at least exponentially decay in t.

It is worth observing that as $\delta \to \pi/2$ the right-hand side of inequality (5.5) tends to ∞. This is in agreement with the fact that heating above in the bidispersive case for a horizontal layer is always stable.

We observe that in the case of an inclined layer heated from below, it is possible to obtain a global nonlinear stability result following the estimates given in [22]. A global stability condition that may be obtained is the following

$$R^2 < \min(1, K_r^{-1}) \frac{\pi^2}{2(1 + \sin \delta)}.$$

6. Numerical results and conclusions

In this section, we present the results for the numerical solution of (4.1)–(4.3), when the layer is heated from below. We employ the Chebyshev tau method and allow for minimization in both a and b to find the minimum value $Ra = R^2$. In this section, we take $\sigma_f = 1$. We have employed other values of σ_f and the variation in the results is not significant. However, the bidispersive parameter K_r plays a strong role as we report below.

Figures 1 and 2 show the critical surfaces in the (a, b, Ra) space, i.e. the surface defined implicitly by $c(a, b, Ra) = 0$ (c is the time evolution exponent, see equation (4.2)), for various angles of
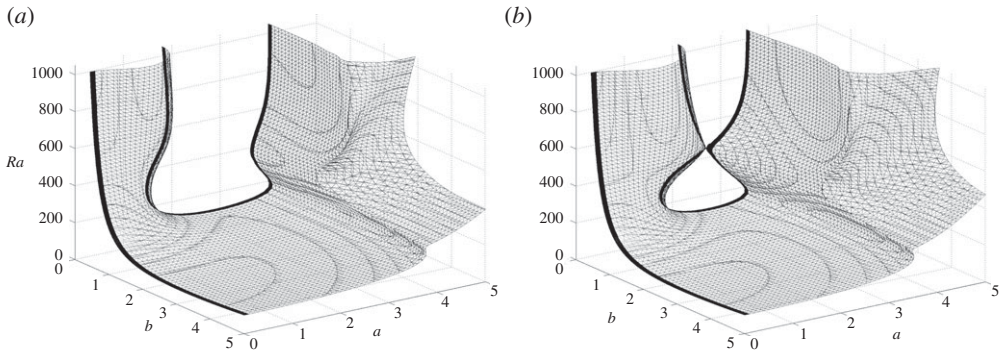
(a)

(b)

Figure 1. Critical surface in the (a, b, Ra) space (i.e. the locus of triplets (a, b, Ra) such that $c = 0$ is an eigenvalue of problem (4.1)–(4.3)) for inclinations $\varphi = 15°$ (a) and $\varphi = 16.255°$ (b). The system is unstable ($c > 0$) 'inside' the surface (e.g. for $a = 2, b = 3, Ra = 400$). The thick lines mark the intersection of the surface with the planes $a = 0$ (longitudinal modes) and $b = 0$ (transverse modes). For $\varphi = 16.255°$, the critical curve for the longitudinal modes (plane $a = 0$) is unchanged, whereas the transverse mode critical curve is almost divided into two disconnected lines. Relative permeability is $K_r = 10^{-4}$.
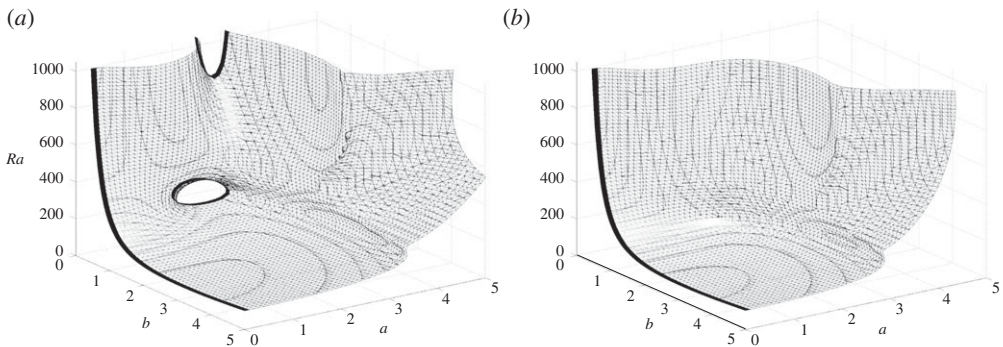
(a)

(b)

Figure 2. Same surfaces as in figure 1 for $\varphi = 17°$ (a) and $\varphi = 20°$ (b). For $\varphi = 17°$, the transverse mode critical curve is considerably reduced and composed of two disconnected lines. For $\varphi = 20°$, transverse modes are stable for any a and Ra (no intersection with the $b = 0$ plane).

inclination ($\varphi = \pi/2 - \delta$). These surfaces are analogous to the critical curves, such as those of figure 4, when we have to consider the two wavenumbers a, b instead of just a. We see that for all angles of inclination, once $\varphi > 0$, the lowest value for Ra is found when $a = 0$, $b = \pi$ (the minimum of Ra on the black line on the plane $a = 0$), so the most unstable convection cells are longitudinal rolls. This is what we might expect, because the same is true for inclined convection in the classical problem employing Darcy's law, cf. e.g. Rees *et al.* [23, p. 16]. In figure 1, the surface of instability touches the plane $b = 0$. In figure 2 with $\varphi = 17°$, there is still an intersection with $b = 0$, but the intersection is reduced. Once $\varphi \gtrsim 17.52°$ (as in figure 2, with $\varphi = 20°$), there is no intersection at all with the plane $b = 0$, so all perturbations in the form of transverse rolls are stable.

Figure 3 shows the critical Rayleigh number values versus the inclination angle φ for various values of $K_r = K_p/K_f$. The transverse mode curves finish abruptly as shown, because there is a critical angle where any instability owing to transverse rolls disappears. This is in complete agreement with the work of Rees & Bassom [24] and the classical inclined Darcy convection problem. Figure 3 demonstrates that the critical Rayleigh number corresponding to longitudinal rolls coincides with that for transverse rolls when $\varphi = 0$ but is lower immediately when $\varphi > 0$ (*this means instability occurs via longitudinal rolls*). Figures 4 and 5 show the behaviour of Ra versus a for transverse rolls when $K_r = 10^{-4}$ for various angles φ. This behaviour is in agreement with

8

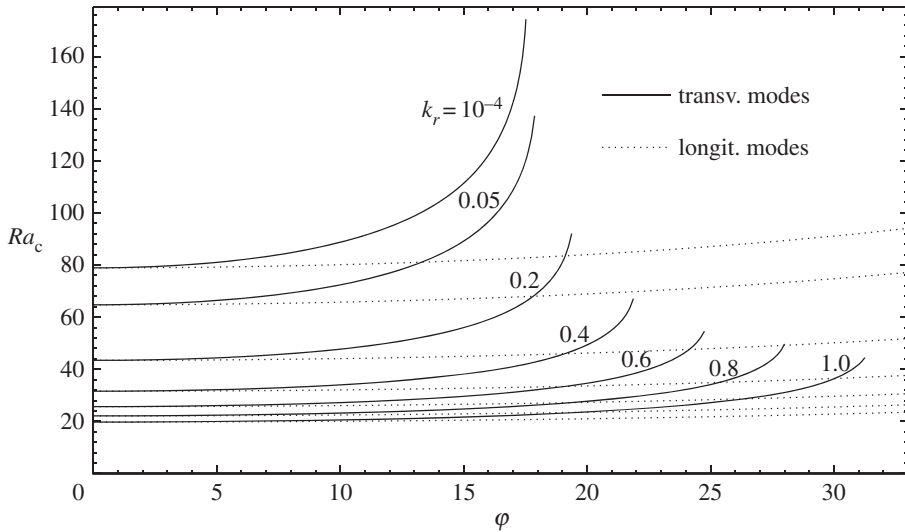rspa.royalsocietypublishing.org *Proc. R. Soc. A* **472**: 20160480

Figure 3. Critical values of Rayleigh number Ra for longitudinal and transverse modes versus angle of inclination φ for various values of K_r. Critical Ra for longitudinal modes is obtained analytically in formula (6.3).
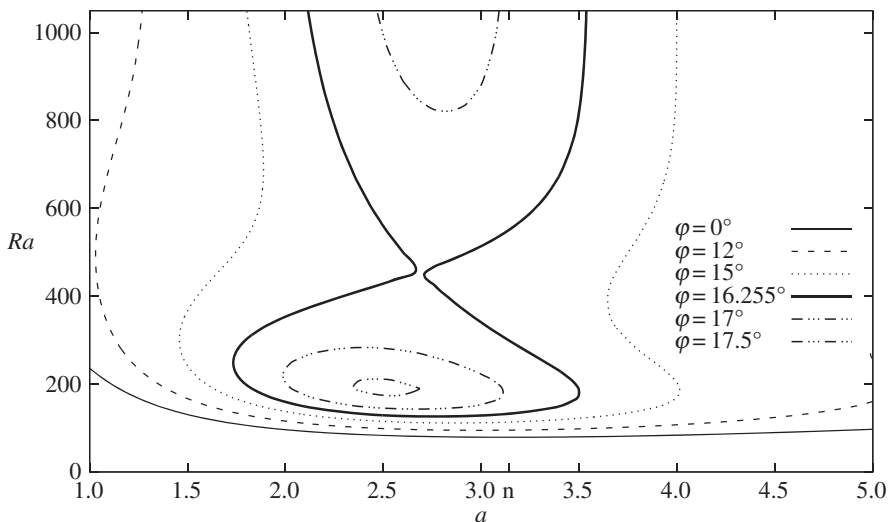

Figure 4. Critical Rayleigh number versus a for transverse modes for various angles of inclination (and $K_r = 10^{-4}$). Curves for $\varphi = 15°$, $\varphi = 16.255°$ and $\varphi = 17°$ can be seen also in figures 1 and 2 on the plane $b = 0$.

that reported for the single porosity case by Rees & Bassom [24]. As is seen from figure 4, a disconnected and closed instability curve forms once φ exceeds 16.255°. Figure 5 shows how this curve behaves as φ increases beyond 17°. A numerical analysis shows that the upper unbounded part of the critical curve shown in figure 5 disappears for some $\varphi < 17.5°$, whereas the lower closed curve persists at least for $\varphi \approx 17.52°$. The same qualitative behaviour is found for other values of K_r, so all the transverse mode curves in figure 3 are continuous until their end. We find (for $K_r = 10^{-4}$) no instability by a transverse mode once $\varphi \gtrsim 17.52°$.

While longitudinal modes do yield the linear instability boundary, it may be that this problem resembles more problems of parallel shear flow, where more than the leading eigenvalue influences the global stability scenario, cf. Straughan [25, ch. 8].
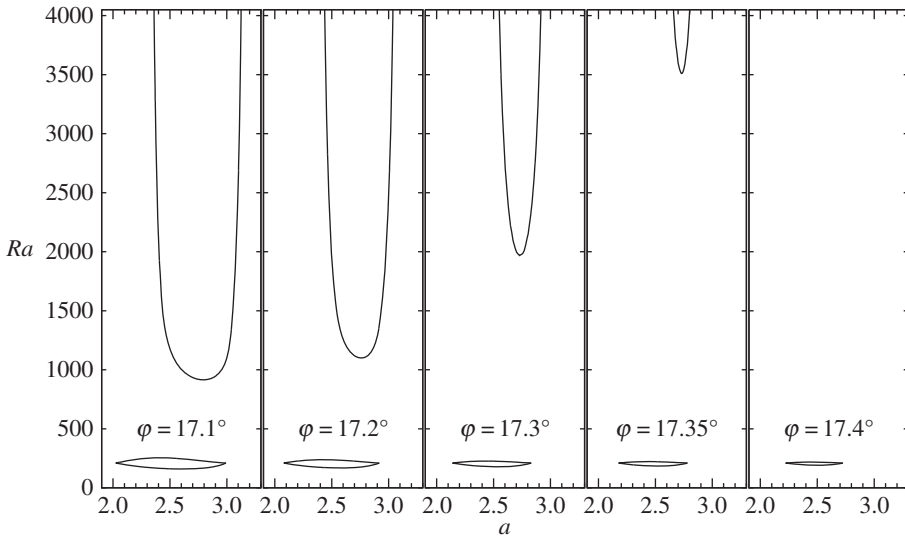
9

rspa.royalsocietypublishing.org *Proc. R. Soc. A* **472**: 20160480

Figure 5. Same parameters of figure 4. Critical Rayleigh number versus a for φ close to value where curve disappears.

To make a direct comparison with the work of Rees & Bassom [24], we take $K_r = 1$ and then form the sum of equations $(3.1)_1$ and $(3.1)_2$. This yields a system of equations of the form

$$-v_i - \tilde{\pi}_{,i} + 2R\lambda_i\theta = 0$$

and

$$c\theta \pm Rv_3 \mp 2R^2 \cos\delta(\tfrac{1}{2} - z)\theta_{,x} = \Delta\theta, \tag{6.1}$$

where $v_i = u_i^f + u_i^P$, $v_3 = w^f + w^P$. Make the transformation $\psi = \sqrt{2}\theta$ and $S = \sqrt{2}R$ and then (6.1) become

$$-v_i - \tilde{\pi}_{,i} + S\lambda_i\psi = 0$$

and

$$c\psi \pm Sv_3 \mp S^2 \cos\delta(\tfrac{1}{2} - z)\psi_{,x} = \Delta\psi. \tag{6.2}$$

System (6.2) is equivalent to the one of Rees & Bassom [24] (their equations (3.2) and (3.3)) and so we take $S^2 = Ra_1 = 2R^2 = 2\,Ra$. Thus, the Rayleigh number reported here is one half of the number reported by Rees & Bassom [24]. We find the angle when instability disappears when $K_r = 1$ is $\approx 31.25°$, which agrees with [24]. We do find that the bidispersive case is very different from the simple porosity case as figure 3 indicates. In fact, for longitudinal rolls equations (4.1)–(4.3) may be solved analytically to yield

$$Ra_{\text{crit}} = R^2 = \frac{2 + K_r}{1 + 5K_r}\frac{4\pi^2}{\sin\delta}. \tag{6.3}$$

Denote by Z the quantity $(2 + K_r)/(1 + 5K_r)$. Then, the critical eigenfunctions w^f, w^P and θ are given by

$$w^P = \frac{2 - Z}{1 + Z}w^f,$$

$$\theta = \frac{3R}{2\pi^2(1 + Z)}w^f,$$

where

$$w^f = \sin\pi z.$$

Clearly, the relative permeability, K_r, is playing a key role in determining the forms of w^f, w^P and θ at the onset of instability. It is worth pointing out that we found no overstability numerically.

By checking the error coefficient τ, we have found that any complex eigenvalues which arise are associated with spurious eigenvalues.

References

1. Chen Y-M, Pearlstein AJ. 1989 Stability of free-convection flows of variable-viscosity fluids in vertical and inclined slots. *J. Fluid Mech.* **198**, 513–541. (doi:10.1017/S0022112089000236)

2. Barletta A. 2015 A proof that convection in a porous vertical slab may be unstable. *J. Fluid Mech.* **770**, 273–288. (doi:10.1017/jfm.2015.154)

3. Barletta A, Celli M. 2016 Instability of combined forced and free flow in an inclined porous channel. *Int. J. Comp. Methods* **13**, 1640001. (doi:10.1142/S0219876216400016)

4. Barletta A, Storesletten L. 2014 Adiabatic eigenflows in a vertical porous channel. *J. Fluid Mech.* **749**, 778–793. (doi:10.1017/jfm.2014.260)

5. Barletta A, Rees DAS. 2015 Local thermal non-equilibrium analysis of the thermoconvective instability in an inclined porous layer. *Int. J. Heat Mass Transf.* **83**, 327–336. (doi:10.1016/j.ijheatmasstransfer.2014.12.006)

6. Nield DA. 1998 Effects of local thermal non-equilibrium in steady convection processes in saturated porous media: forced convection in a channel. *J. Porous Media* **1**, 181–186.

7. Nield DA. 2002 A note on modelling of local thermal non-equilibrium in a structured porous medium. *Int. J. Heat Mass Transf.* **45**, 4367–4368. (doi:10.1016/S0017-9310(02)00138-2)

8. Nield DA, Bejan A. 2013 *Convection in porous media*. 4th edn. New York, NY: Springer.

9. Nield DA, Kuznetsov AV. 2006 The onset of convection in a bidisperse porous medium. *Int. J. Heat Mass Transf.* **49**, 3068–3074. (doi:10.1016/j.ijheatmasstransfer.2006.02.008)

10. Straughan B. 2015 *Convection with local thermal non-equilibrium and microfluidic effects*. Advances in Mechanics and Mathematics, vol. 32. Berlin, Germany: Springer.

11. Nield DA. 2016 A note on the modelling of bidisperse porous media. *Transp. Porous Media* **111**, 517–520. (doi:10.1007/s11242-015-0607-5)

12. Zuber A, Motyka J. 1998 Hydraulic parameters and solute velocities in triple-porosity karstic-fissured-porous carbonate aquifers—case-studies in southern Poland. *Environ. Geol.* **34**, 243–250. (doi:10.1007/s002540050276)

13. Ghasemizadeh R, Hellweger F, Butscher C, Padilla I, Vesper D, Field M, Alshawabkeh A. 2012 Review: groundwater flow and transport modeling of karst aquifers, with particular reference to the North Coast Limestone aquifer system of Puerto Rico. *Hydrogeol. J.* **80**, 1441–1461. (doi:10.1007/s10040-012-0897-4)

14. Huang T, Guo X, Chen F. 2015 Modelling transient flow behaviour in a multiscale triple porosity model for shale gas reservoirs. *J. Nat. Gas Sci. Eng.* **23**, 33–46. (doi:10.1016/j.jngse.2015.01.022)

15. Kim J, Moridis GJ. 2015 Numerical analysis of fracture propagation during hydraulic fracturing operations in shale gas systems. *Soc. Petrol. Eng. J.* **76**, 127–137. (doi:10.1016/j.ijrmms.2015.02.013)

16. Montrasio L, Valentino R, Losi GL. 2011 Rainfall infiltration in a shallow soil: a numerical simulation of the double-porosity effect. *Electron. J. Geotechnol. Eng.* **16**, 1387–1403.

17. Sanavia L, Schrefler BA. 2012 Finite element analysis of the initiation of landslides with a non-isothermal multiphase model. In *Mechanics, models and methods in civil engineering* (eds M Frémond, F Maceri), Lecture Notes in Applied Computational Mechanics, vol. 61, pp. 123–146. Berlin, Germany: Springer.

18. Hammond NP, Barr AC. 2014 Global resurfacing of Uranus's moon Miranda by convection. *Geology* **42**, 931. (doi:10.1130/G36124.1)

19. Joseph DD. 1976 *Stability of fluid motions*, vol. 2. Berlin, Germany: Springer.
20. Straughan B 2008 *Stability and wave motion in porous media*. Applied Mathematical Sciences, vol. 165. New York, NY: Springer.
21. Dongarra JJ, Straughan B, Walker DW. 1996 Chebyshev tau algorithm methods for calculating spectra of hydrodynamic stability problems. *Appl. Numer. Math.* **22**, 399–435. (doi:10.1016/S0168-9274(96)00049-9)
22. Falsaperla P, Giacobbe A, Lombardo S, Mulone G. 2016 Stability of hydromagnetic laminar flows in an inclined heated layer. *Ric. Mat.* In press. (doi:10.1007/s11587-016-0290-z)
23. Rees DAS, Postelnicu A, Storesletten L. 2006 The onset of Darcy–Forchheimer convection in inclined porous layers heated from below. *Transp. Porous Media* **64**, 15–23. (doi:10.1007/s11242-005-1396-z)
24. Rees DAS, Bassom AP. 2000 The onset of Darcy–Benard convection in an inclined layer heated from below. *Acta Mech.* **144**, 103–118. (doi:10.1007/BF01181831)
25. Straughan B. 1998 *Explosive instabilities in mechanics*. Heidelberg, Germany: Springer.

11

rspa.royalsocietypublishing.org *Proc. R. Soc. A* **472**: 20160480